Electronic Supplementary Information

Schiff base caped gold nanoparticles for transition metal ions sensing in organic media

Miroslava Čonková,[a,b#] Verónica Montes-García,[c#] Marcin Konopka,[a,b] Artur Ciesielski,[c] Paolo Samori,*[c] and Artur R. Stefankiewicz*[a,b]*

a. Faculty of Chemistry, Adam Mickiewicz University, Uniwersytetu Poznańskiego 8, 61-614 Poznań, Poland. E-mail: ars@amu.edu.pl

b. Center for Advanced Technologies, Adam Mickiewicz University, Uniwersytetu Poznańskiego 10, 61-614 Poznań, Poland.

c. Université de Strasbourg, CNRS, ISIS, 8 alleé Gaspard Monge, 67000 Strasbourg, France.

# These authors contributed equally to this work

Table of Contents

Experimental section

Chemicals. Chemicals were purchased from commercial suppliers (Sigma-Aldrich and TriMen Chemicals) and used as received without further purification.

Characterization techniques. NMR spectroscopic data were performed on a Bruker UltraShield 300 MHz and 600 MHz spectrometers, calibrated against the residual protonated solvent signal (for ^{1}H NMR DMSO-d_6: $\delta = 2.50$; $CDCl_3$: $\delta = 7.26$ for ^{13}C NMR DMSO-d_6: $\delta = 39.52$) and are given in ppm. ESI-MS spectra were recorded on a Bruker Impact HD Q-TOF spectrometer in positive ion mode. IR spectra were obtained with a Jasco 4000 FTIR spectrophotometer, and peak positions are reported in cm^{-1}. UV–vis spectra were recorded on a Jasco V-750 UV–visible spectrophotometer. The size of AuNPs was determined through transmission electron microscopy (TEM) analysis in a Hitachi H 7500 microscope operating at an acceleration voltage of 100 kV and by dynamic light scattering (DLS) using a Zetasizer Nano S (Malvern Instruments, Malvern UK). For ICP-MS experiments concentrated HNO_3 (Suprapur, Merck, Germany) was used to prepare the blank samples, calibration standards and as a digestion reagent. Concentrated HCl (Suprapur, Merck, Germany) was used to prepare the blank samples and calibration standards. A single element Ni (Merck, Germany) standard solution of 1000 mg L^{-1} concentration and a multi-elemental standard solution STD-4 (Perkin-Elmer, USA) containing 10 mg L^{-1} Au were used to prepare the set of calibration standards with concentrations: 0.1, 1, 10, 50 μg L^{-1} in 1% HNO3 and 1% HCl for Ni and Au, respectively. Milli-Q water was used to prepare sample dilutions, blank samples and calibration standards (Direct-Q 3 UV, Merck, Germany). The ICP-MS model 7700x (Agilent, USA) operated in no-gas mode, the isotopes ^{58}Ni and ^{197}Au were measured with the following instrumental settings: Seaspray nebulizer 0.2 mL min-1, Scott double pass spray chamber,

0.1 s dwell times per isotope, 100 sweeps, 3 replicates, 1550 W plasma power and 1.05 mL min-1 nebulizer gas flow rate. The 2 min wash-in time was applied for Au measurement before each standard and sample to reduce the potential memory effects.

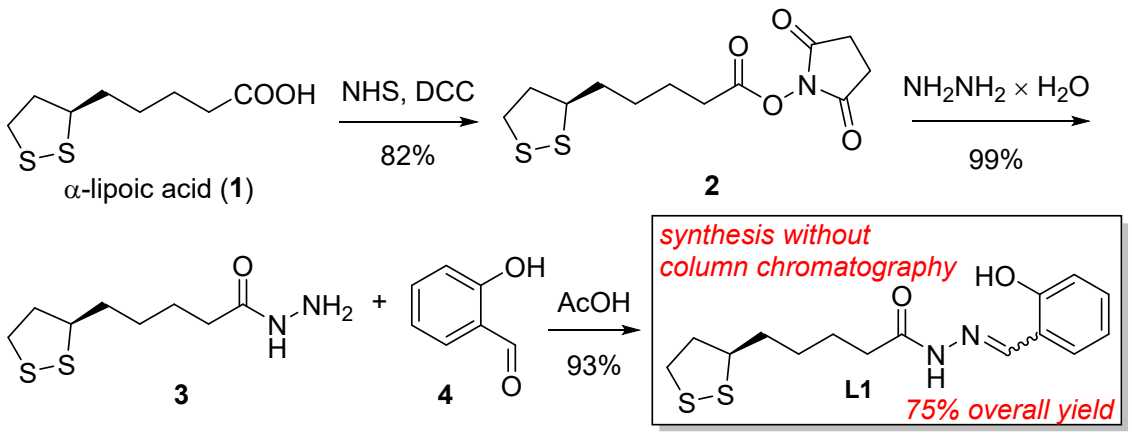

Synthesis of L1:

Scheme S1 *Reagents and conditions*: i) NHS, DCC, CH_2Cl_2, 0°C to rt, 3 h; ii) $NH_2NH_2 \times H_2O$, CH_2Cl_2, rt, 17 h; iii) AcOH, EtOH, rt, 17 h.

Active Ester 2: NHS (308 mg, 2.65 mmol, 1.1 equiv.) was added to a stirring solution of α-lipoic acid (500 mg, 2.4 mmol, 1 equiv.) in dry CH_2Cl_2 (10 mL) under an argon atmosphere and at room temperature. The resulting mixture was cooled to 0 °C by an ice-water bath and a solution of DCC (550 mg, 2.65 mmol, 1.1 equiv.) in dry CH_2Cl_2 (3 mL) was added dropwise. A few seconds after the addition of DDC solution, a white precipitate of DCU started to appear. The cooling bath was removed, and the reaction mixture was allowed to warm up to room temperature, while stirring, for 3 hours. After that, the white solid of DCU was filtered through a small pad of silica and the solvent was removed under reduced pressure. The residue was then purified via recrystallization in a mixture of chloroform (3 mL) and *n*-hexane (100 mL) to give rise to the active ester **2** (600 mg, 1.98

mmol, 82 %), as a white solid. **2**: ^{1}H NMR (600 MHz, DMSO-d_6): δ 1.41-1.52 (m, 2H), 1.54-1.75 (m, 4H), 1.85-1.93 (m, 1H), 2.38-2.46 (m, 1H), 2.68 (t, 2H, J = 7.2 Hz), 2.81 (s, 4H), 3.12 (dt, 1H, J = 6.8 Hz, J = 11.0 Hz), 3.16-3.23 (m, 1H), 3.57-3.66 (m, 1H). ^{13}C NMR (151 MHz, DMSO-d_6): δ 24.0, 25.4, 27.6, 30.0, 33.8, 38.1, 39.8, 55.9, 168.9, 170.2. The physical and spectral data are consistent with those reported.[1]

Hydrazide 3: An excess of hydrazine monohydrate (0.35 mL, 7.16 mmol, 4 equiv.) was added to a stirring solution of the active ester (544 mg, 1.79 mmol, 1 equiv.) in dry CH_2Cl_2 (15 mL). The resulting mixture was stirred at room temperature for 17 hours, after it was quenched with water (40 mL) and extracted with CH_2Cl_2 (3 × 50 mL). The combined organic layers were washed with brine (100 mL) and dried over anhydrous Na_2SO_4. After filtration, the solvent was removed under reduced pressure. Et_2O (5 mL) was added to the residue to precipitate the compound 3, which was then filtered (pale-yellow solid, 394 mg, 1.78 mmol, 99%). Compound 3 should be stored in the fridge under an argon atmosphere. **3**: ^{1}H NMR (600 MHz, DMSO): δ 1.29-1.38 (m, 2H), 1.44-1.74 (m, 4H), 1.82-1.91 (m, 1H), 2.01 (t, 2H, J = 7.4 Hz), 2.37-2.45 (m, 1H), 3.11 (dt, 1H, J = 6.8 Hz, J = 11.0 Hz), 3.16-3.21 (m, 1H), 3.56-3.63 (m, 1H), 4.14 (bs, 2H), 8.91 (bs, 1H). ^{13}C NMR (151 MHz, DMSO): δ 25.0, 28.3, 33.2, 34.1, 38.1, 39.9, 56.1, 171.4. The physical and spectral data are consistent with those reported.[2]

Ligand L1: To a stirring suspension of hydrazide **3** (100 mg, 45.4 μmol, 1 equiv.) in absolute EtOH (10 mL), salicylaldehyde **4** (50 μL, 45.4 μmol, 1 equiv.) and a catalytic amount of acetic acid (0.25 mL) were added. The resulting mixture was stirred for 2 hours at room temperature. After that, the solvent was removed under reduced pressure and to the residue, Et_2O (5 mL) was added to precipitate ligand L1 as a white solid, which was then

filtered (137 mg, 42.2 μmol, 93%). **L1:** mp = 122-123 °C; FT-IR (ATR) ν_{max} = 3186, 3080, 2926, 2849, 1666, 1605, 1580, 1461, 1396, 1206, 770 cm^{-1}; ^{1}H NMR (600 MHz, DMSO): δ 1.34–1.47 (m, 2H), 1.53–1.75 (m, 4H), 1.83–1.92 (m, 1H), 2.23 + 2.58 (2 t, 2H, *J* = 7.3 Hz), 2.36–2.45 (m, 1H), 3.07–3.15 (m, 1H), 3.15–3.22 (m, 1H), 3.58–3.66 (m, 1H), 6.83–6.93 (m, 2H), 7.20–7.30 (m, 1H), 7.49 + 7.61 (2 d, 1H, *J* = 7.5 Hz), 8.25 + 8.34 (2 s, 1H), 10.12 (s) + 11.12–11.25 (m, 1H), 11.12–11.25 (m) + 11. 58 (s, 1H).^{13}C NMR (151 MHz, DMSO): δ 23.9, 24.7, 28.3, 28.4, 31.8, 33.8, 34.1, 34.2, 38.1 (2x), 39.9, 56.1 (2x), 116.1, 116.3, 118.6, 119.2, 119.4, 120.0, 126.7, 129.4, 130.8, 131.1, 140.8, 146.4, 156.3, 157.3, 168.3, 173.7. HRMS – (ESI) calc for $C_{15}H_{21}N_2O_2S_2^+$ $[M+H]^+$ 325.1039, found 325.1042.

MS and FT-IR characterization of L1:

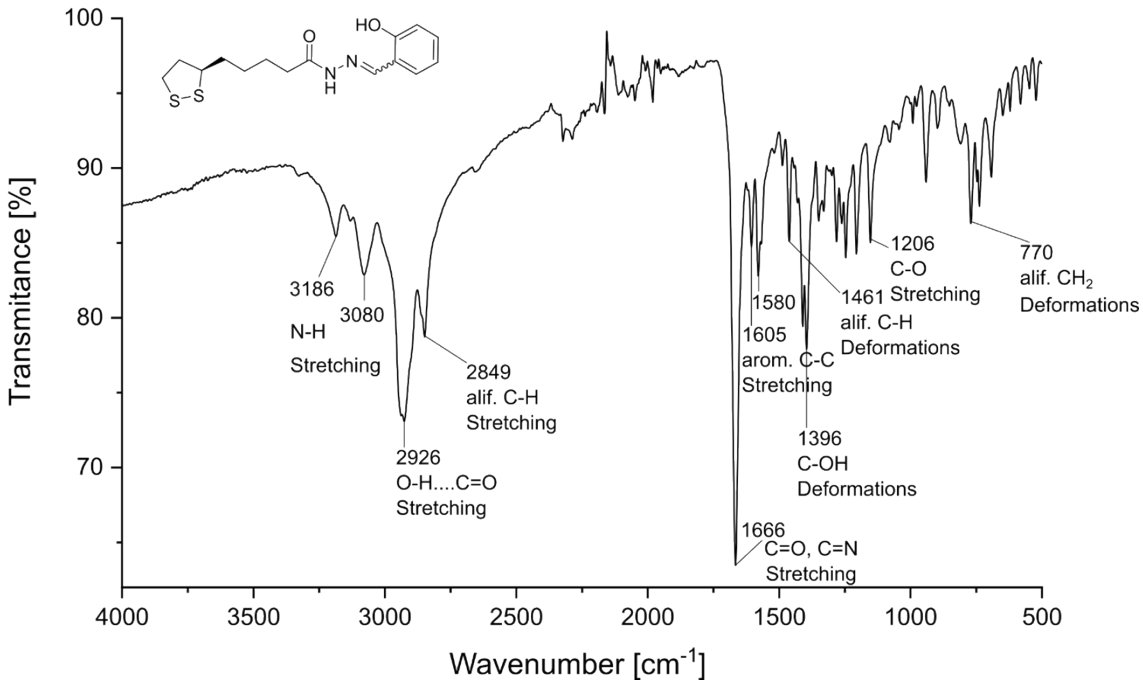

Figure S1. FT-IR (ATR) spectrum of ligand **L1.**

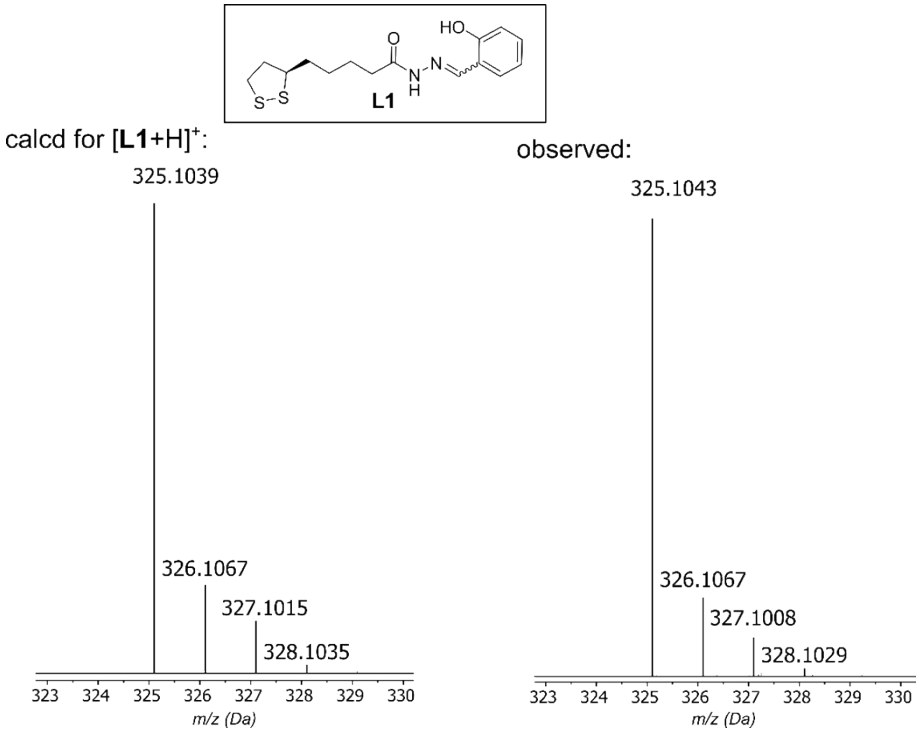

Figure S2. ESI-MS spectra (in positive mode) of ligand **L1.** Calculated on the left and observed on right.

1D and 2D NMR Spectra of L1

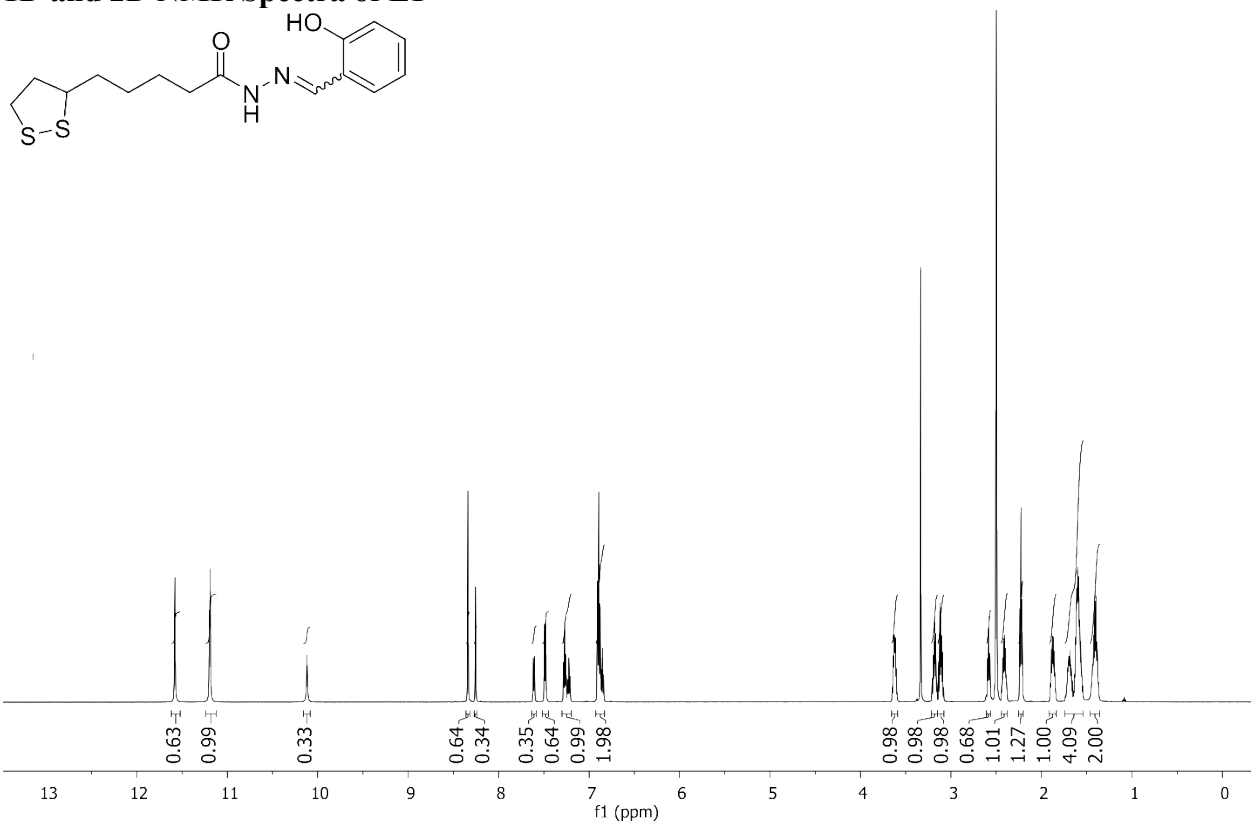

Figure S3. ^{1}H NMR spectrum (600 MHz, DMSO) of ligand **L1**.

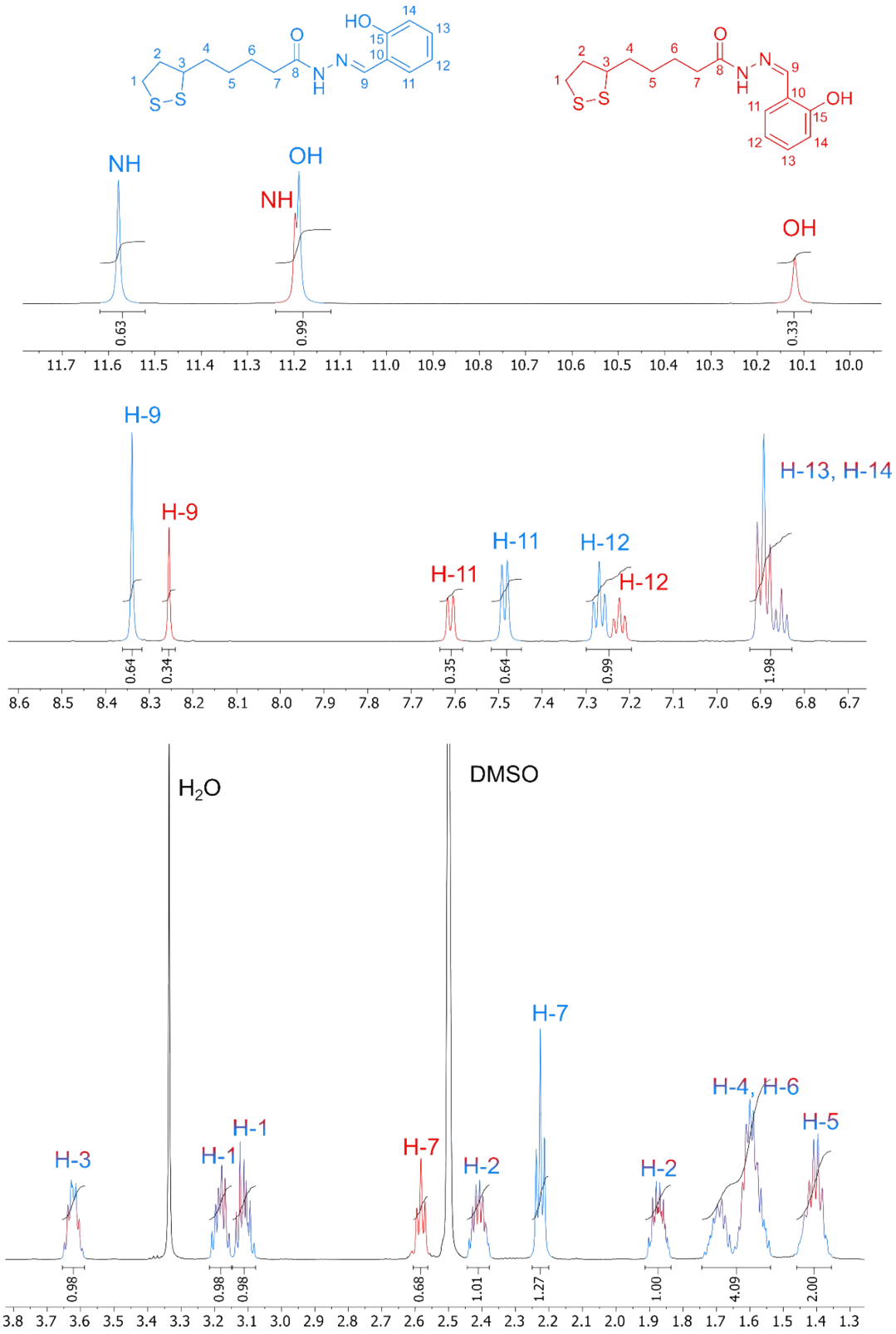

Figure S4. Zoomed areas from ^{1}H NMR spectrum (600 MHz, DMSO) of ligand **L1** with proton assignment (according to 1D and 2D NMR).

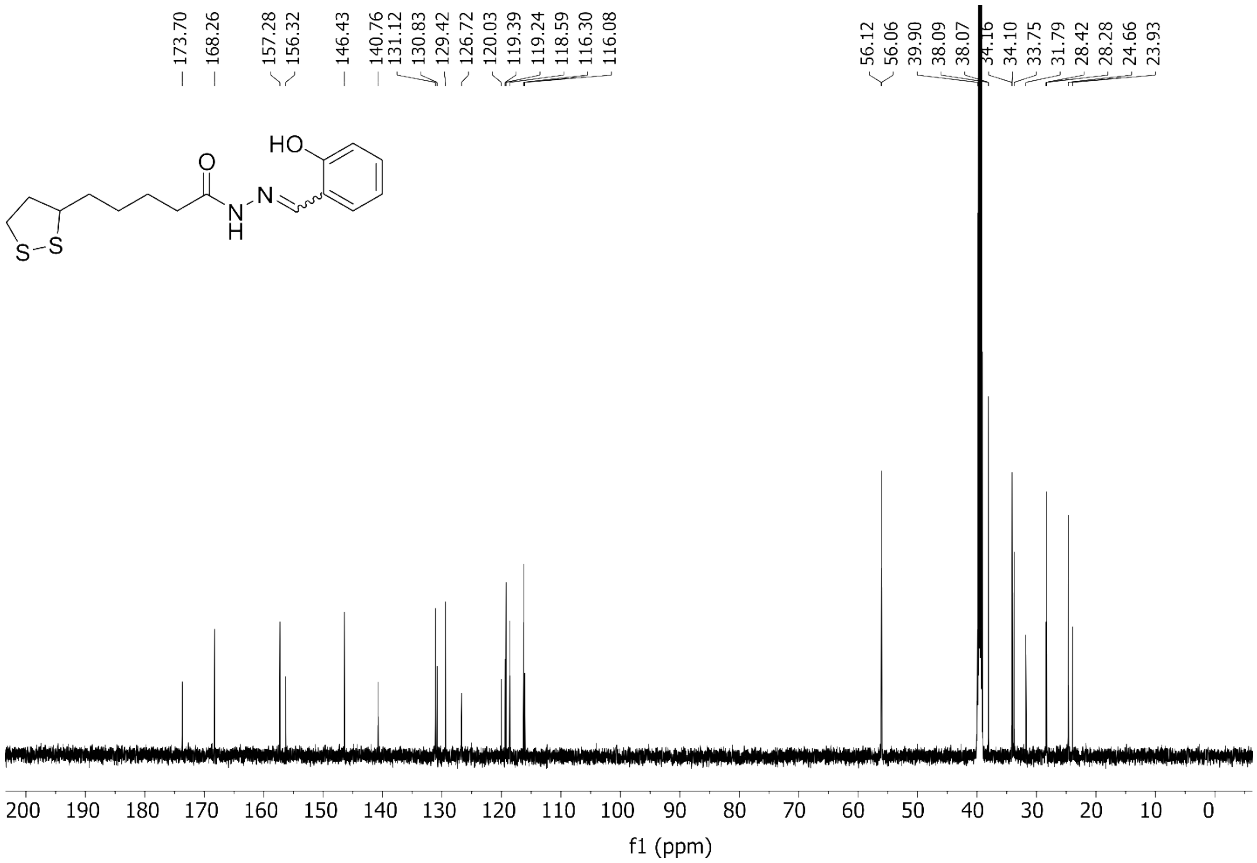

Figure S5. ^{13}C NMR spectrum (151 MHz, DMSO) of ligand **L1**.

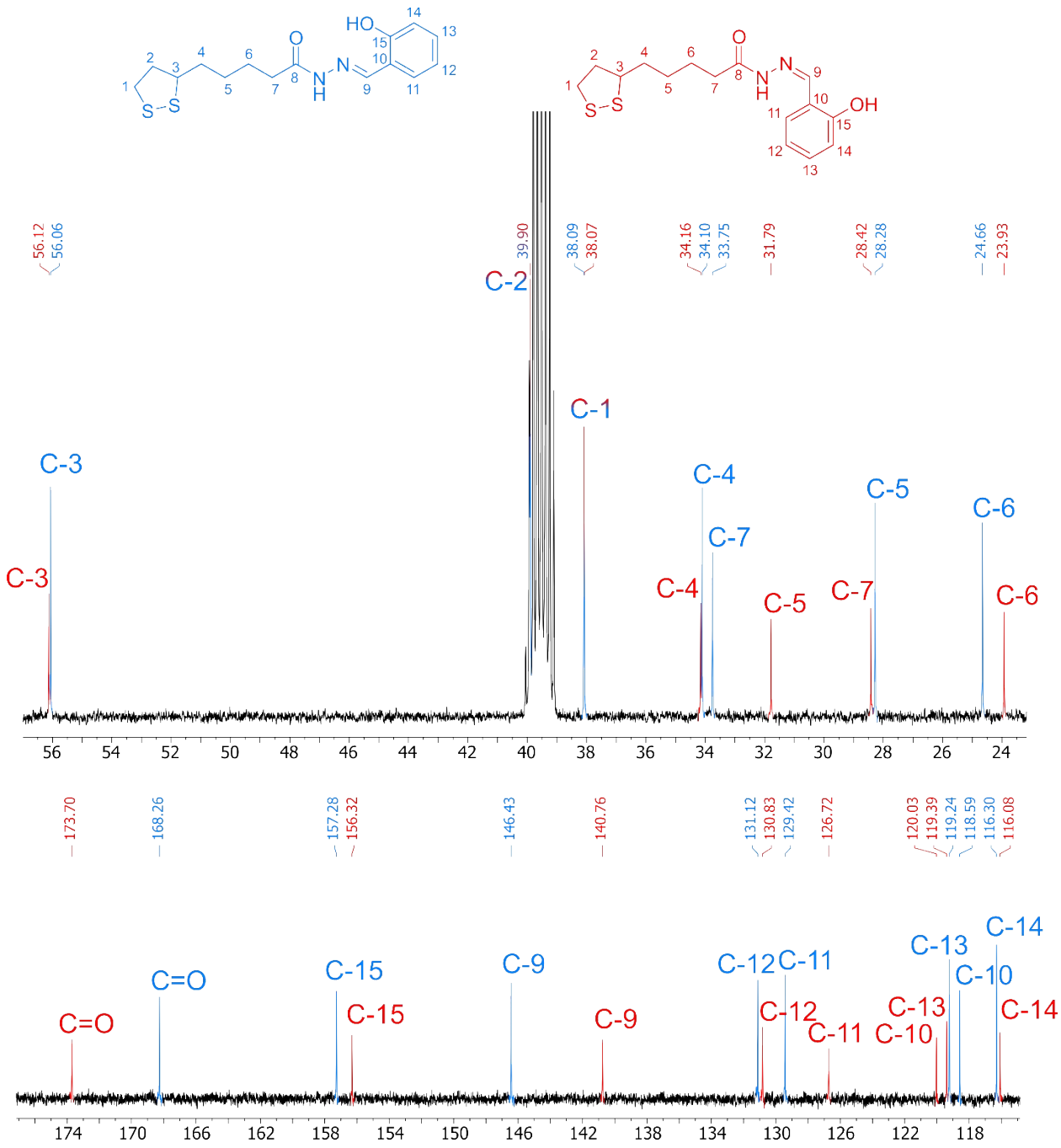

Figure S6. Zoomed areas from ^{13}C NMR spectrum (151 MHz, DMSO) of ligand **L1** with carbon assignment (according to 1D and 2D NMR).

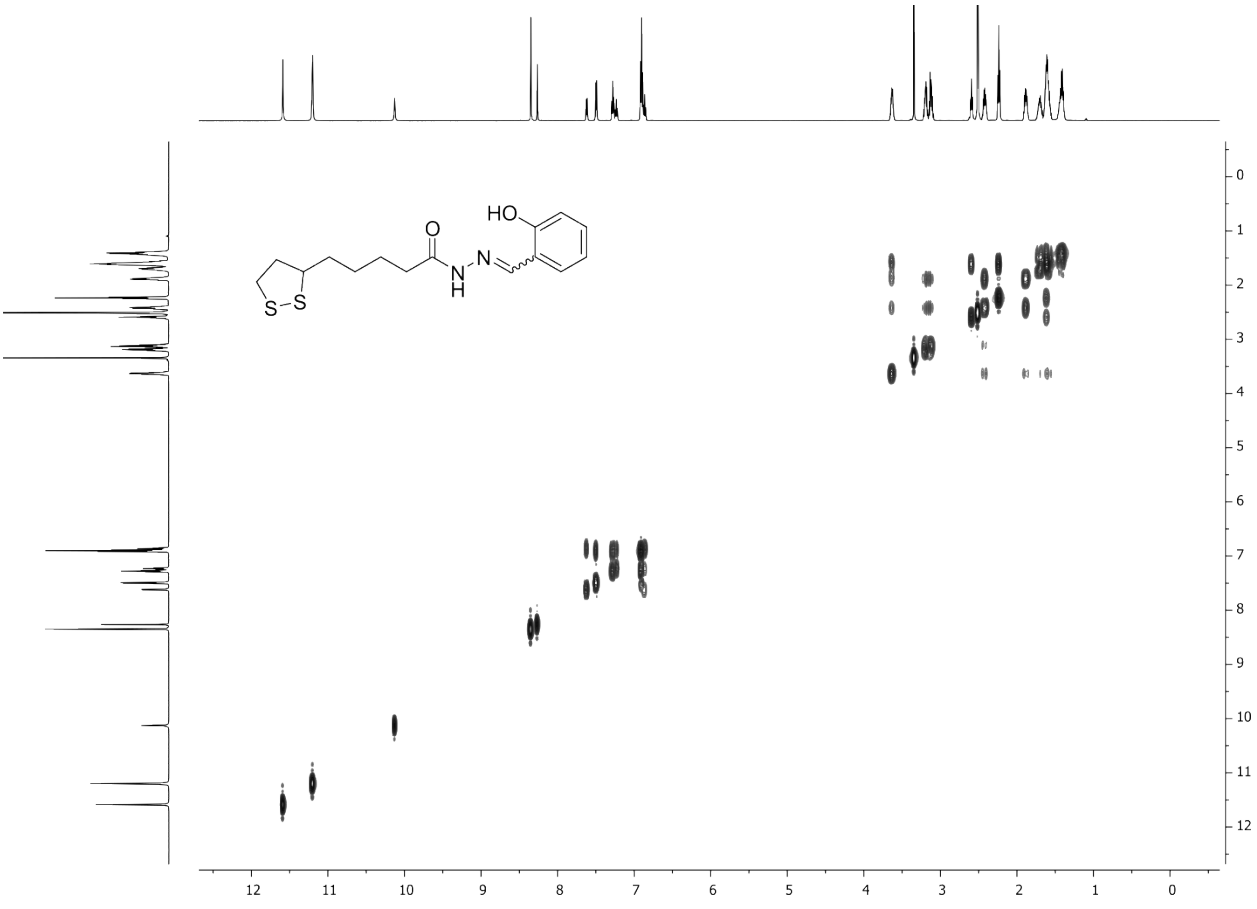

Figure S7. ^{1}H-^{1}H COSY NMR spectrum (600 MHz, DMSO) of ligand **L1**.

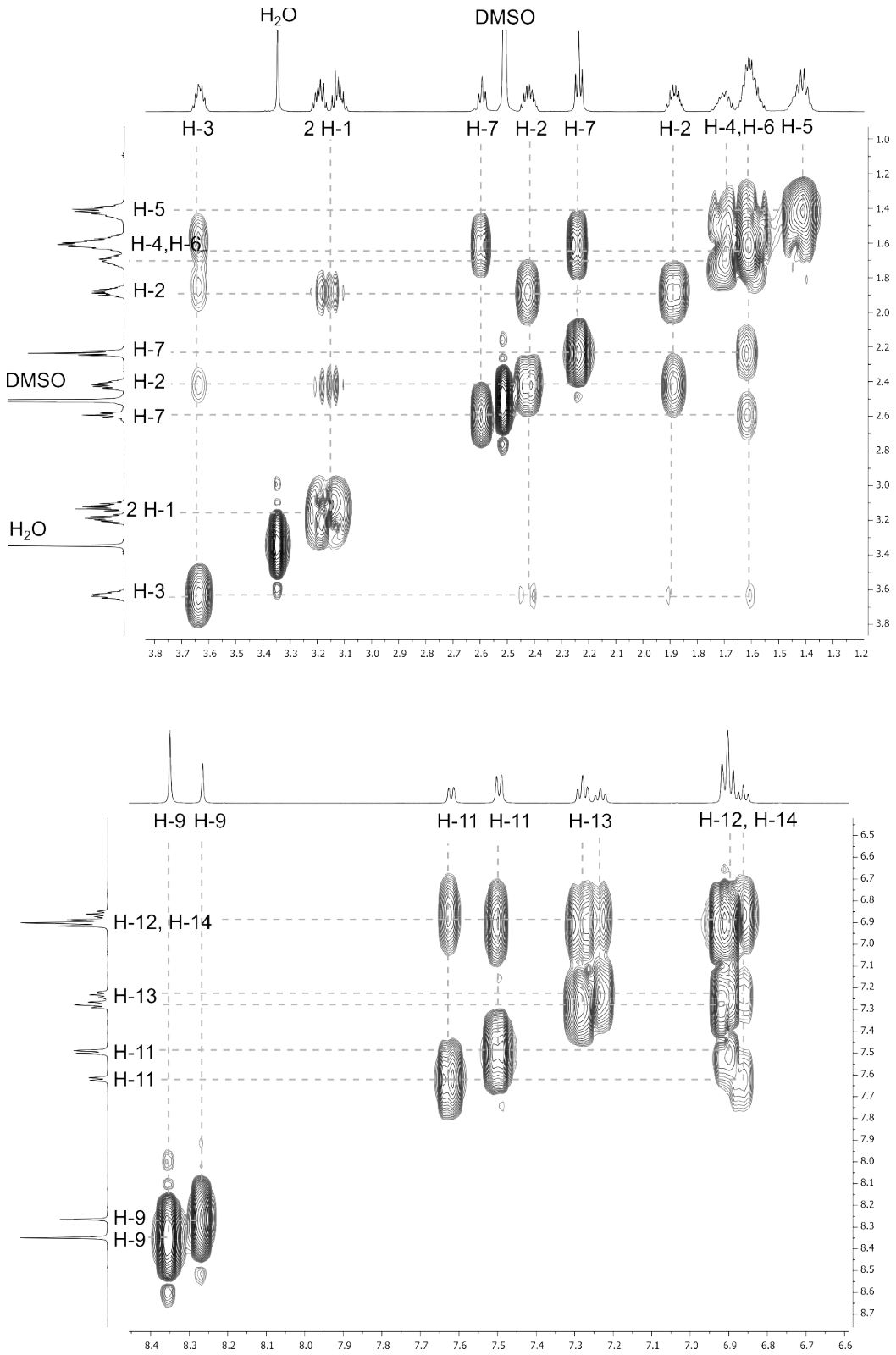

Figure S8. Zoomed areas from ^{1}H-^{1}H COSY NMR spectrum (600 MHz, DMSO) of ligand **L1** with proton assignment (according to 1D and 2D NMR).

Synthesis of L2:

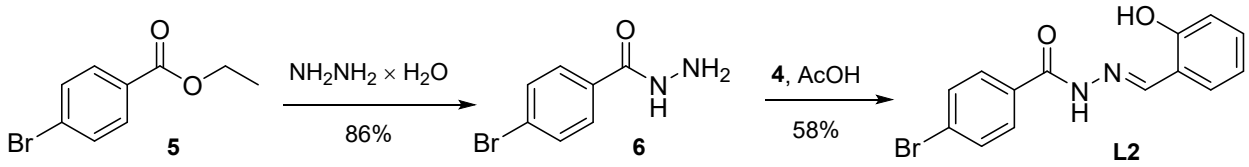

Scheme S2 *Reagents and conditions*: i) $NH_2NH_2 \times H_2O$, EtOH, reflux, 5 h; ii) AcOH, EtOH, 65 °C, 0.5 h.

Hydrazide 6: Hydrazine **6** was prepared according to a previously reported procedure.[3] To a solution of ethyl 4-bromobenzoate **5** (5 g, 21.8 mmol, 1 equiv.) in EtOH (10 mL), hydrazine monohydrate (4 mL, 82.2 mol, 3.8 equiv.) was added in one portion. The mixture was stirred under reflux for 5 hours. After cooling down to room temperature, distilled water was added (15 mL). The precipitated product was filtered and washed with distilled H_2O. Compound 6 was isolated as white solid (4.02 g, 18.7 mmol, 86%). **6**: ^{1}H NMR (300 MHz, DMSO): δ 4.51 (bs, 2H), 7.65 (d, 2H, J = 8.6 Hz), 7.76 (d, 2H, J = 8.6 Hz), 9.86 (bs, 1H). ^{13}C NMR (75 MHz): δ 124.8, 129.1, 131.4, 132.4, 164.9. The physical and spectral data are consistent with those reported.[4]

Ligand L2: To a stirring suspension of hydrazide **6** (1.85 g, 8.6 mmol, 1 equiv.) in absolute EtOH (50 mL), salicylaldehyde **4** (0.9 mL, 8.6 mmol, 1 equiv.) and a catalytic amount of acetic acid (0.15 mL) were added. The resulting mixture was stirred for 30 minutes at 65 °C. Ligand L2 (1.59 g, 5.0 mmol, 58%) was then collected as white crystals by filtration and dried under vacuum. **L2**: ^{1}H NMR (300 MHz, DMSO): δ 6.90–6.95 (m, 2H), 7.28–7.34 (m, 1H), 7.56 (d, 1H, J = 7.7 Hz), 7.77 (d, 2H, J = 8.6 Hz,), 7.89 (d, 2H, J = 8.6 Hz), 8.65 (bs, 1H), 11.21 (bs, 1H), 12.17 (bs, 1H). ^{13}C NMR (75 MHz): δ 116.4, 118.7, 119.4, 125.8, 129.4, 129.7, 131.5, 131.6, 131.9, 148.4, 157.5, 161.9. The physical and spectral data are consistent with those reported.[5]

1D NMR Spectra of L2

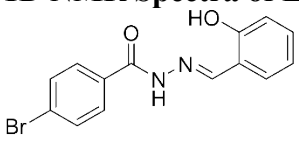

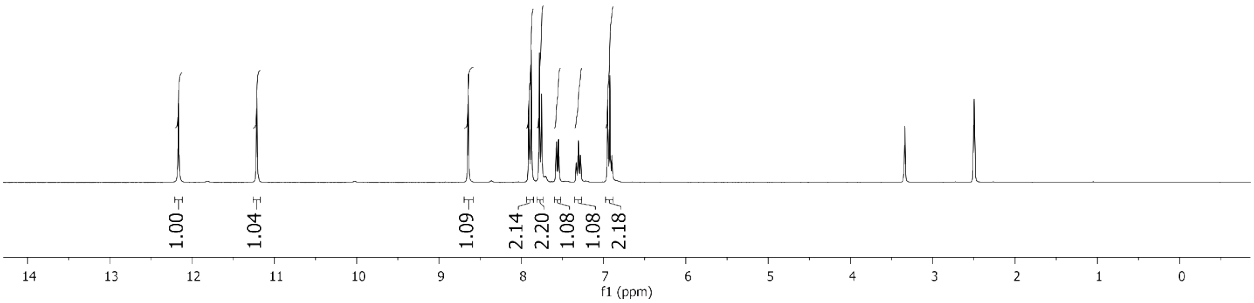

Figure S9. ^{1}H NMR spectrum (300 MHz, DMSO) of ligand **L2**.

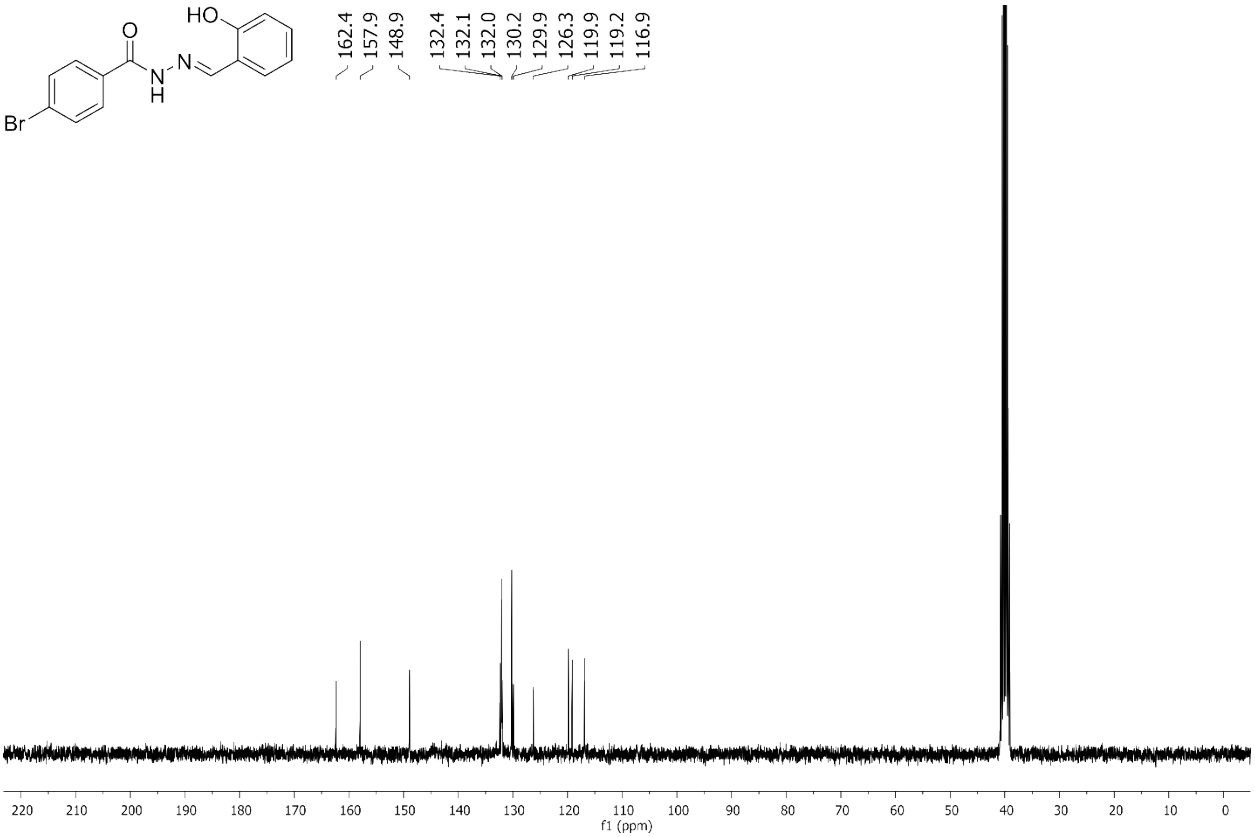

Figure S10. ^{13}C NMR spectrum (75 MHz, DMSO) of ligand **L2**.

To evaluate the effectiveness of the proposed chelating system in the coordination of the selected d-electron metal ions, ligand **L2**, in which the α-lipoic acid moiety was replaced by a –Br group, was also synthesized (Scheme S2, Fig. S9 and S10). This structural change was implemented to avoid potential competing reactions between metal ions and the unbound lipoic acid moiety, which is known to form complexes via disulphide–metal interaction.[6, 7] Complexation reactions of **L2** with several transition metal ions (Fe^{3+}, Cu^{2+}, Ni^{2+}, all as nitrate salts) were conducted in acetonitrile, followed by recrystallization of the products by addition of diethyl ether. Based on the assumptions that the ligand would function as a tridentate chelate and that the chosen metal ions would adopt octahedral coordination, the reaction mixtures were composed with an M:L2 ratio of 1 : 2. This has

been confirmed by mass spectrometry, where signals consistent with the presence of $[M(L2)_2]$ (M=Cu, Ni) and $[M(L2)_2]+$ (M=Fe) species have been found (Fig. S11).

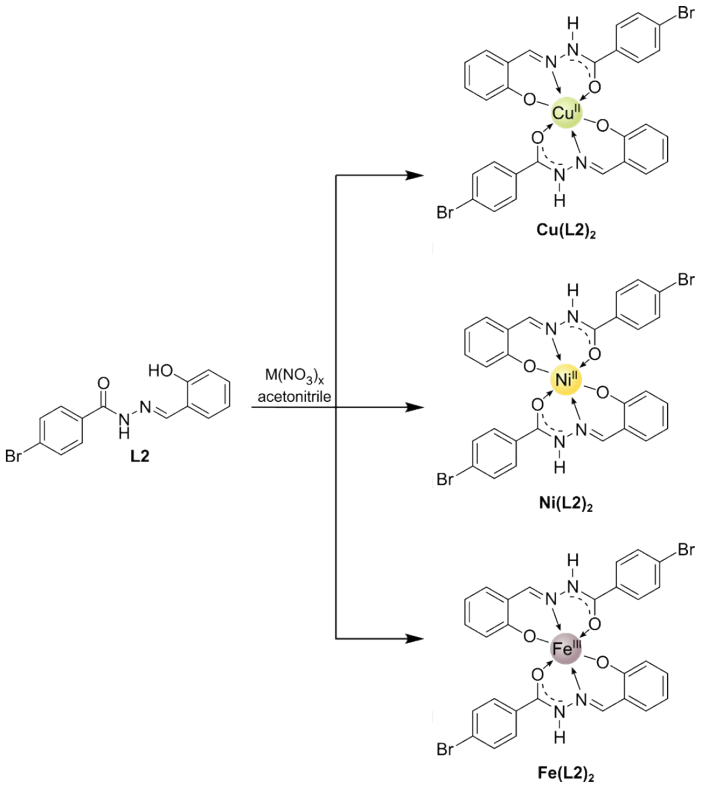

Scheme S3 Schematic representation of **$Cu(L2)_2$**, **$Ni(L2)_2$** and **$Fe(L2)_2$** synthesis.

General procedure for the complex (L2-Mx+) preparation: To the suspension of **L2** (50 mg, 0.156 mmol) in acetonitrile (5 mL) a metal salt (0.078 mmol, 0.5 equiv.) was added. The mixture was stirred for 24 hours at room temperature. After that, the solvent was evaporated, and the product was recrystallized from CH_3CN/Et_2O mixture to obtain the product (71-85 %).

MS Spectra of Complexes $Cu(L2)_2$, $Ni(L2)_2$ and $Fe(L2)_2$

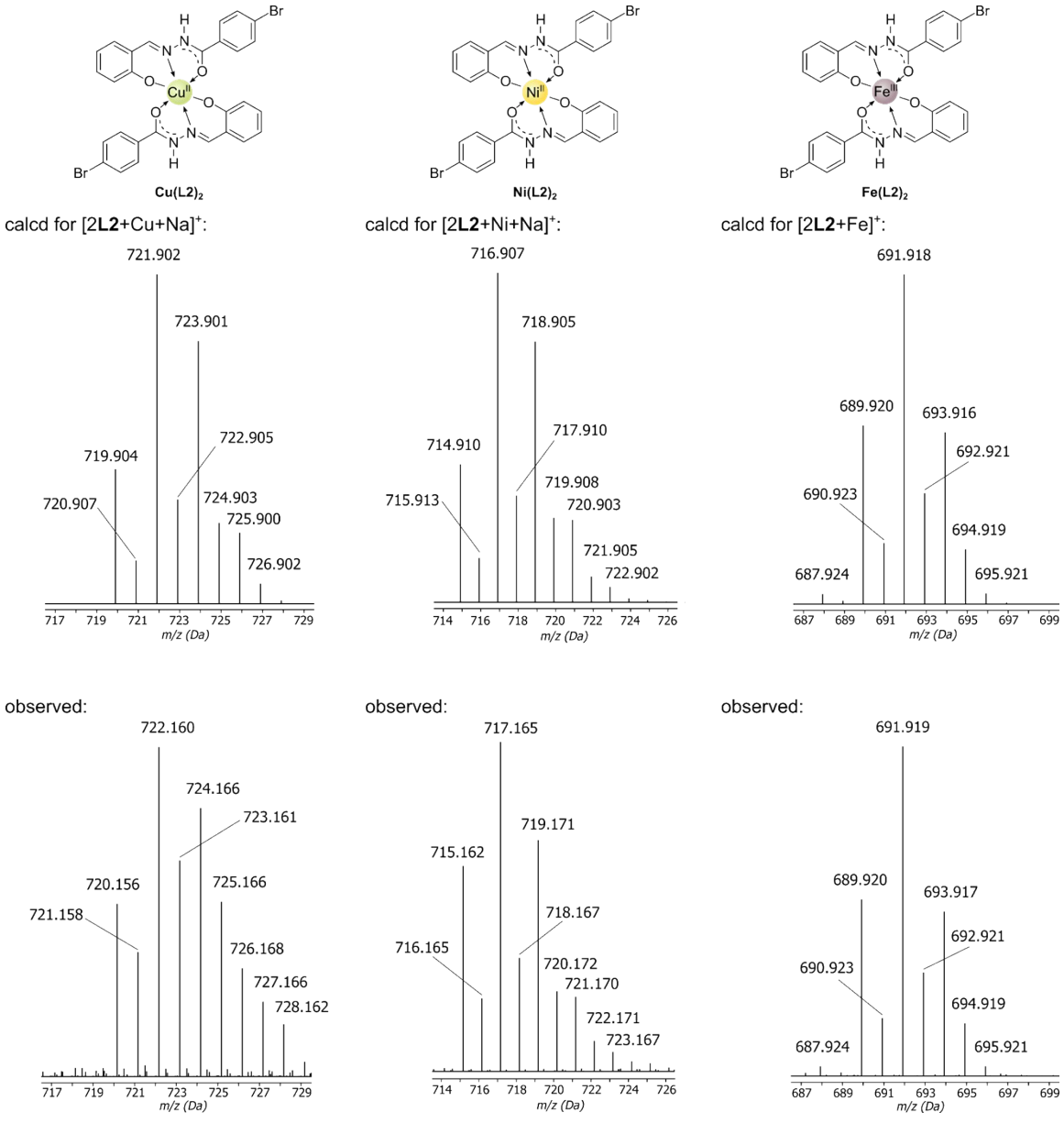

Figure S11. ESI-MS spectra (in positive mode) of complexes **$Cu(L2)_2$**, **$Ni(L2)_2$** and **$Fe(L2)_2$.** Calculated on top and observed on the bottom.

Synthesis of gold nanoparticles

Gold nanoparticles were synthesized according to a reported procedure.[8] In detail: $HAuCl_4$ $3H_2O$ (50 mg, 0.127 mmol) was dissolved in oleylamine (12.7 mL). The mixture was sonicated for 30 minutes to dissolve $HAuCl_4$ $3H_2O$ completely. Then, the solution was heated at 110 °C under vigorous stirring for 40 minutes. In a few minutes, the initial orange solution turned colourless and short after deep red. After letting the mixture cool down to room temperature, EtOH was added (30 mL) to precipitate the gold nanoparticles. The solution was then centrifuged at 384 RCF for 10 minutes to remove the excess of reactants. Toluene (3 mL) was added to re-disperse gold nanoparticles and then EtOH (20 mL) was added to precipitate the gold nanoparticles again. The solution was centrifuged at 384 RCF (Relative Centrifugal Force) for 10 minutes. This washing procedure was repeated twice. After that, toluene (12.6 mL) was added to prepare a 10 mM solution in terms of a gold metal, which is stable for up to several weeks when stored in the fridge. Au NPs concentration was determined by UV-Vis spectroscopy on the basis of extinction at 400 nm.[9] All glassware was rigorously cleaned in aqua regia before use.

General procedure for ligand exchange reaction:

To roughly estimate the needed amount of ligand **L1** needed for such a reaction we started from purely geometrical considerations: The diameter distribution of our AuNPs, roughly to ~11 nm was determined by transmission electron microscopy (Figure S14). From theoretical and experimental studies on Au/thiolated SAMs, reported the n literature, it is known that the maximum molecular density of alkanethiol SAMs, on flat Au [111], amounts ~ 4.5 molecules/nm^2. [10, 11] By considering the higher steric hindrance of ligand **L1**, compared to aliphatic chains, and

that for particles bigger than 5.2 nm the curvature radius is negligible at molecular scales[10, 12], it is possible to conclude that the upper limit for the density of molecules in the AuNPs-ligand **L1** SAM is equal 4.5 molecules/nm^2. Therefore, each nanoparticle cannot react with more than 890 ligand **L1** molecules. By knowing the concentration, size, and amount of active sites for reaction with the thiols group we could estimate an approximate stoichiometric ratio between AuNPs and ligand **L1** solution to achieve a complete ligand exchange.

These calculations were a quick and useful guide and a start point for finding the right conditions for the ligand exchange. We set up test concentrations of **L1** to 7.5 μM, 15 μM, 30 μM and 60 μM. Stock **OL**@AuNPs solution concentration was set to 1 mM (in toluene, in terms of metal) to form 0.5 mM solution after the addition the same volume of **L1** solution in toluene.

Gold nanoparticles (**OL**@AuNPs) solution in toluene (1 mM in terms of gold metal, 2 mL) was added to a solution of **L1** (7.5-60 μM, 2 mL) in toluene under vigorous stirring. After the addition, the mixture was kept in dark for 96 hours. For the evaluation of the stability UV-Vis measurements were performed in different time intervals (up to 96 hours). The resulting functionalized gold nanoparticles were diluted with toluene to a concentration of 0.25 mM (in terms of gold metal) and further used in the sensing experiments without additional purification steps due to the negligible amount of unbound **L1**.

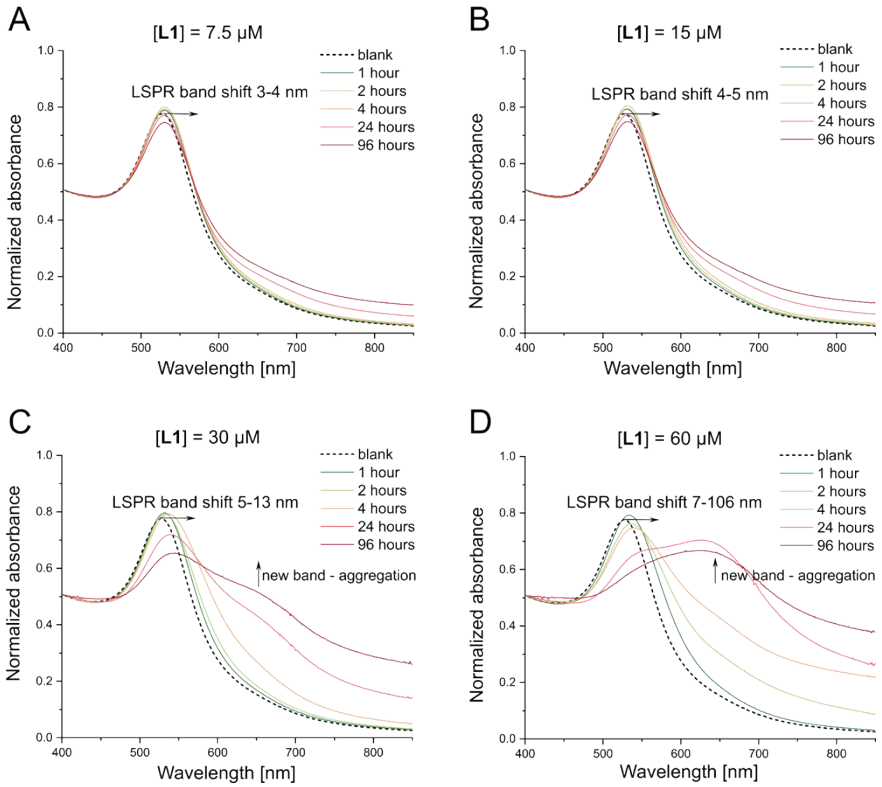

Figure S12. Time-resolved UV-Vis spectra of gold nanoparticles solution (0.25 mM) in toluene upon addition of 7.5 µM (**A**),15 µM (**B**), 30 µM (**C**), 60 µM (**D**) solution of **L1** in toluene. All spectra were normalized at 400 nm to facilitate comparison.

Morphology and Size Determination of Gold Nanoparticles

DLS measurements:

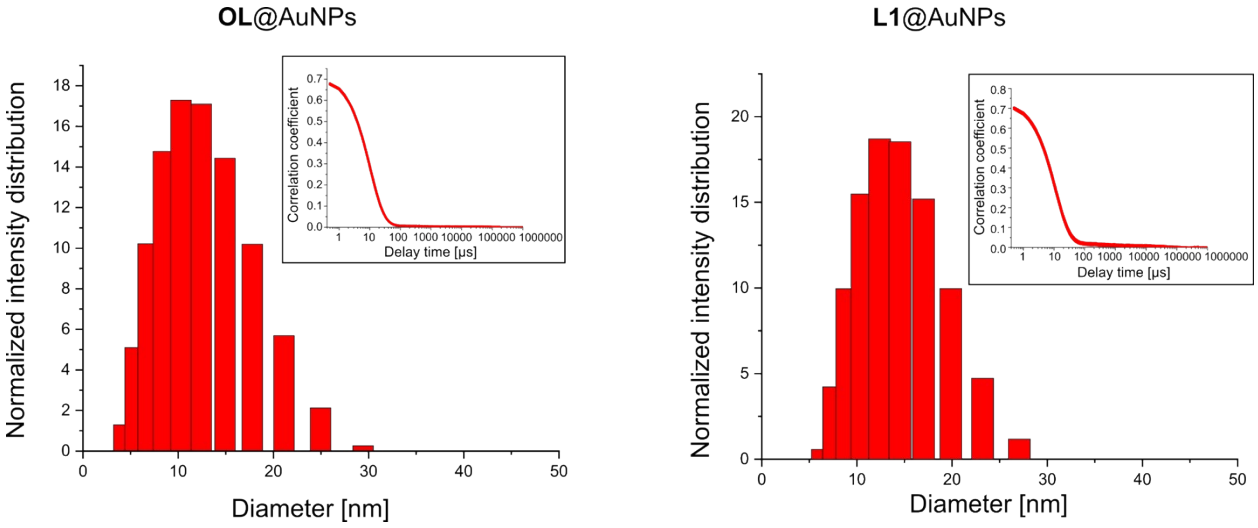

Figure S13. Representative dynamic light scattering (DLS) measurements of gold nanoparticles in toluene solution (0.25 mM) capped with oleylamine (left) showing an average hydrodynamic diameter 14.30 ± 4.38 nm (PdI: 0.186; calculated for n = 5 measurements) and gold nanoparticles in toluene solution (0.25 mM) capped with **L1** (right) showing an average hydrodynamic diameter 15.45 ± 4.26 nm (PdI: 0.243; calculated for n = 5 measurements).

TEM measurements:

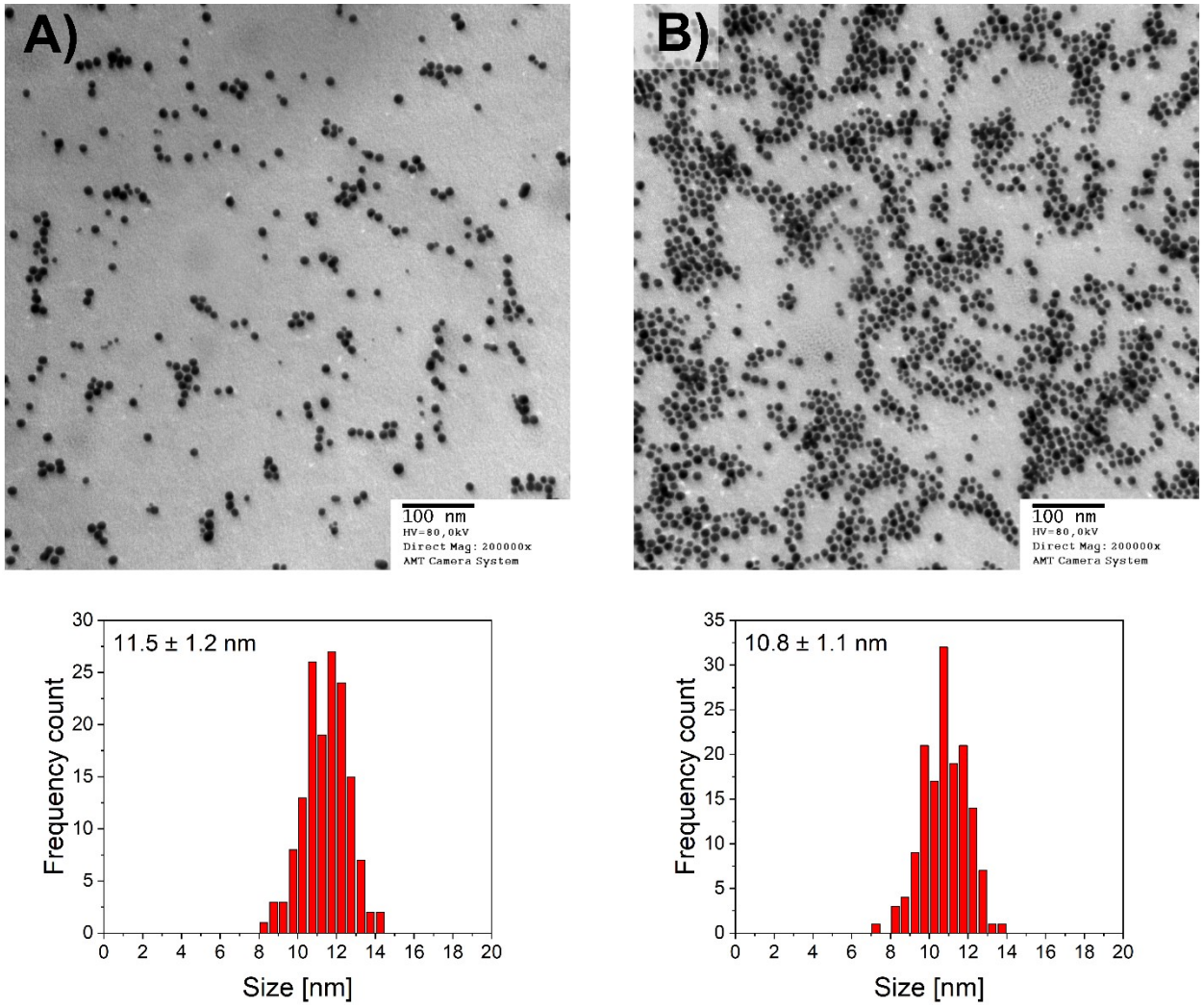

Figure S14. Representative transmission electron microscopy (TEM) images of gold nanoparticles capped by oleylamine (**A**) showing spherical, relatively monodispersed nanoparticles with mean diameter 11.4 ± 1.3 nm, n = 150; and gold nanoparticles capped by ligand **L1** (**B**) showing spherical nanoparticles with mean diameter 10.8 ± 1.1 nm, n = 150.

Sensing metal cations– Cu^{2+}, Ni^{2+}, Fe^{3+}

ICP-MS evaluation of Au content in L1@AuNPs dispersion used for sensing experiments

Sample preparation: 3.5 mL of **L1**@AuNPs dispersion was evaporated under reduced pressure to dryness. To the resulting solid, 1 mL of aqua regia was added and the volume was adjusted to 5 mL with Milli-Q water. The sample for ICP-MS measurement was appropriately diluted. The molar concentration of Au dispersion used for sensing experiments was calculated as 0.246 mM from ICP-MS results (Table S1) following the concentration calculated from UV-vis spectroscopy, 0.25mM.

Table S1. Concentration of Au in **L1**@AuNPs dispersion used for sensing experiments determined by ICP-MS (c = concentration; SD = standard deviation; CV = coefficient of variation).

dilution	c [ug/L]	SD [ug/L]	CV [%]
1000	33 955	246	0.72

General procedure for sensing experiments:

Limit of detection: To 2 mL of gold nanoparticles (in toluene, ~0.25 mM in terms of gold metal) different amounts (20-222 µL, 0.1 mM stock solutions) of metal salts were added. All spectra were measured at room temperature.

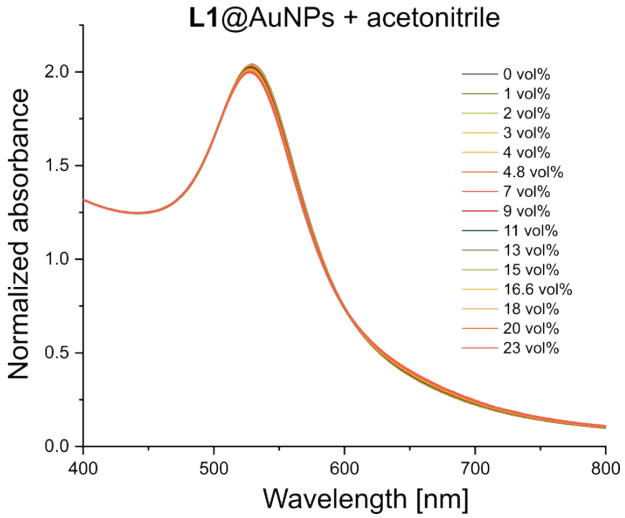

Figure S15. UV-Vis spectra of **L1**@AuNPs upon addition of acetonitrile up to 23 vol%. All spectra were normalized at 400 nm to facilitate comparison.

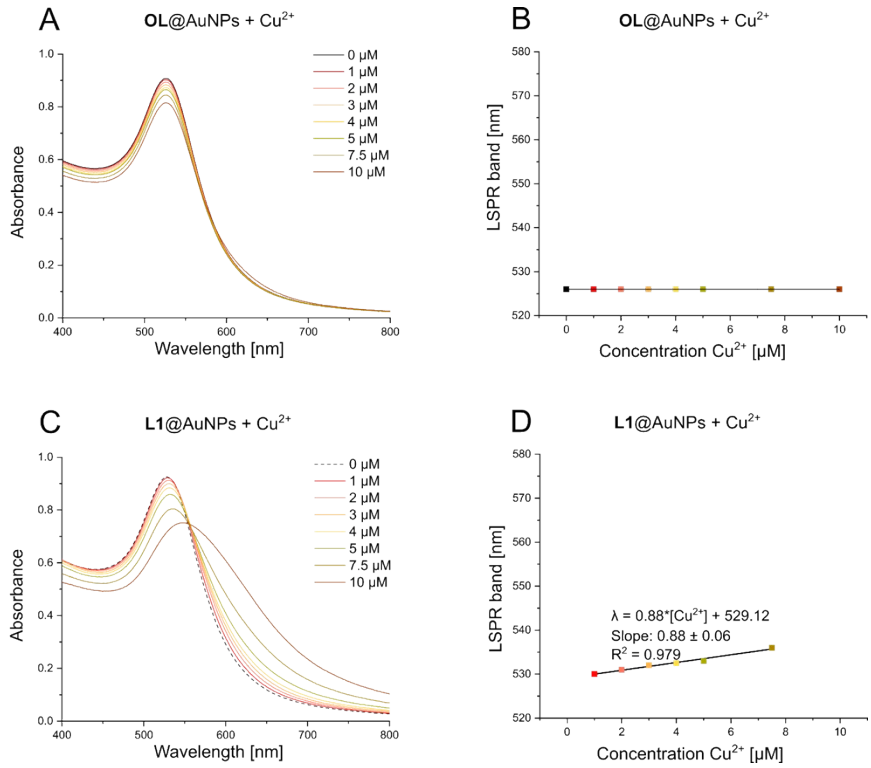

Figure S16. **A** blank experiment: UV-vis spectra of **OL**@AuNPs in toluene upon the addition of $Cu(NO_3)_2$ in acetonitrile; **B** blank experiment: SPR band shift depending on concentration of Cu^{2+} salt; **C** UV-vis spectra of **L1**@AuNPs in toluene upon the addition of $Cu(NO_3)_2$ in acetonitrile; **D** LSPR band shift depending on concentration of Cu^{2+} salt in linear range.

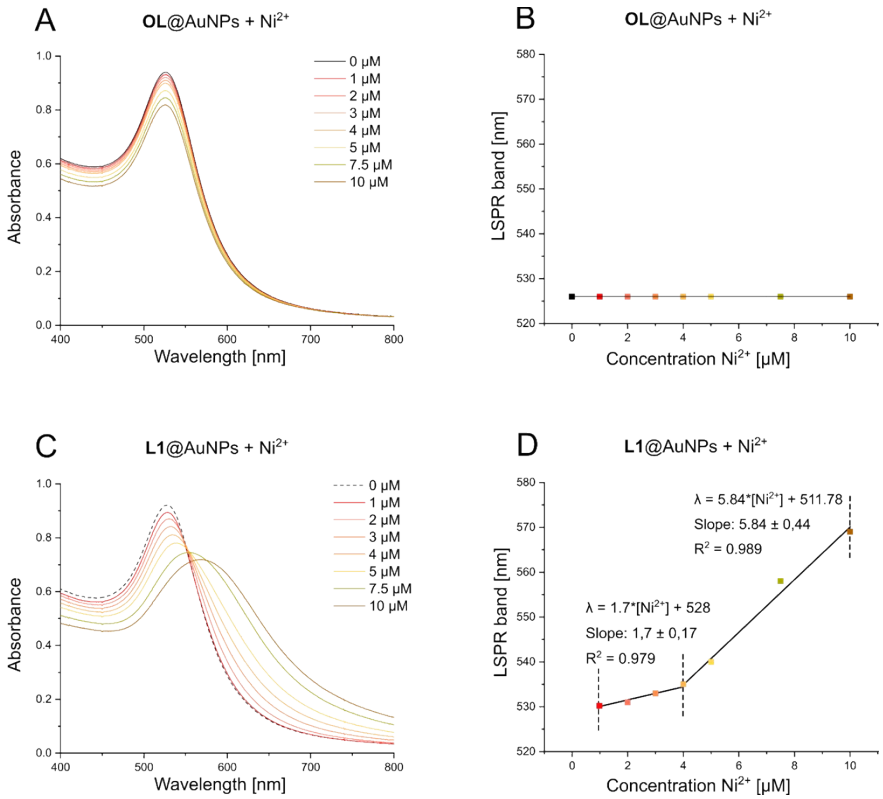

Figure S17. A blank experiment: UV-vis spectra of **OL**@AuNPs in toluene upon increment addition of $Ni(NO_3)_2$ in acetonitrile; **B** blank experiment: SPR band shift depending on concentration of Ni^{2+} salt; **C** UV-vis spectra of **L1**@AuNPs in toluene upon increment addition of $Ni(NO_3)_2$ in acetonitrile; **D** LSPR band shift depending on concentration of Ni^{2+} salt in linear range.

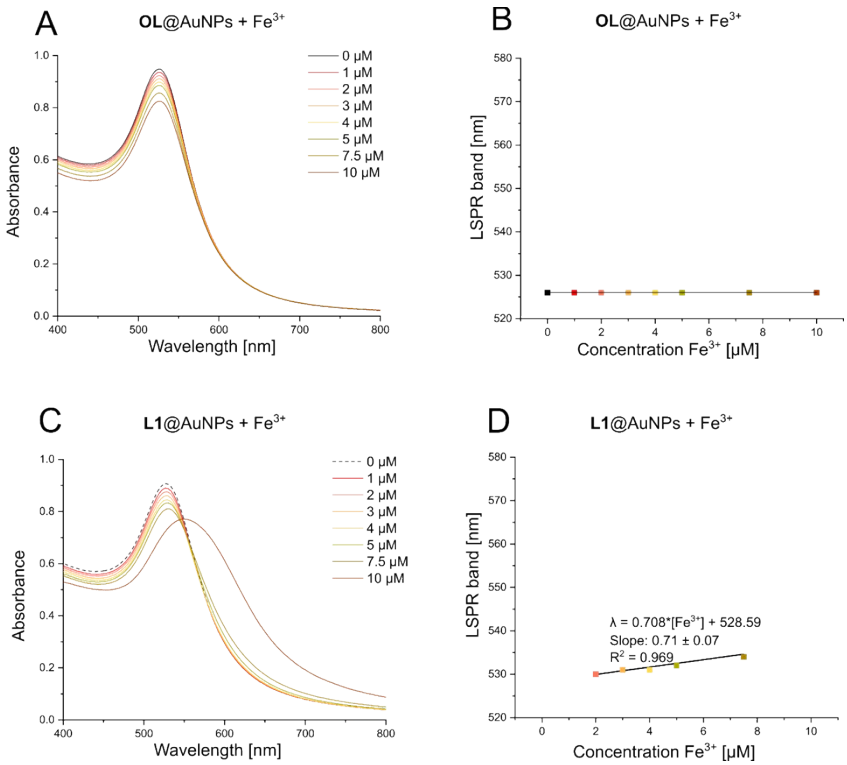

Figure S18. **A** blank experiment: UV-vis spectra of **OL**@AuNPs in toluene upon increment addition of $Fe(NO_3)_3$ in acetonitrile; **B** blank experiment: SPR band shift depending on concentration of Fe^{3+} salt; **C** UV-vis spectra of **L1**@AuNPs in toluene upon increment addition of $Fe(NO_3)_3$ in acetonitrile; **D** LSPR band shift depending on concentration of Fe^{3+} salt in linear range.

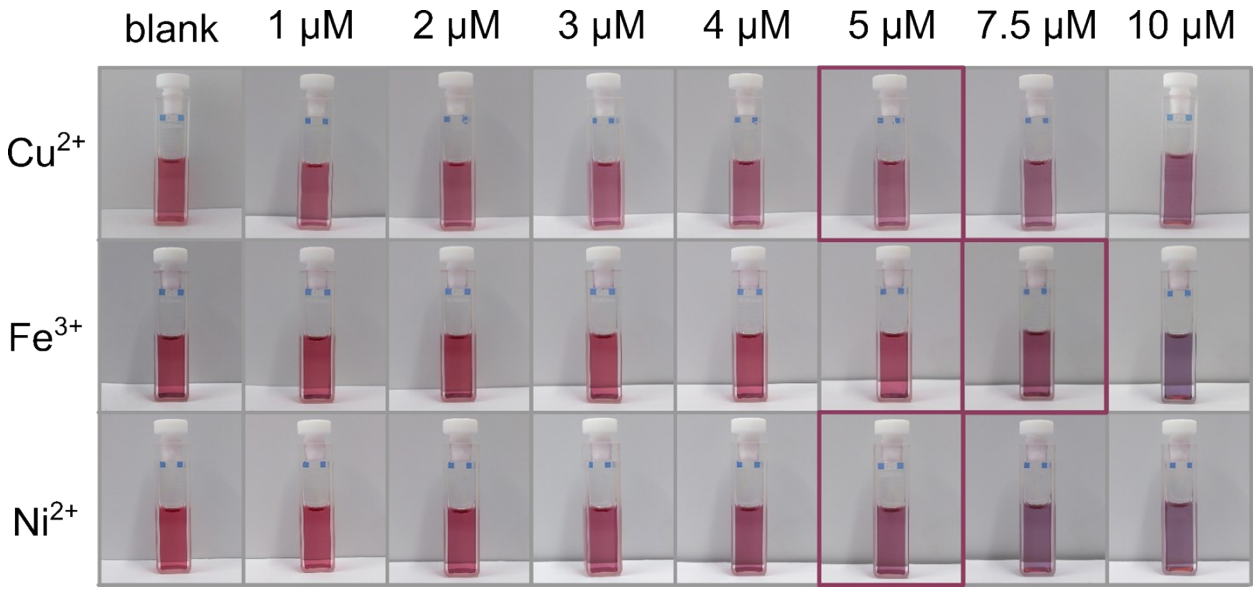

Figure S19. Photographs of **L1**@AuNPs upon incremental addition of transition metal salt solution. Highlighted photographs correspond to the concentration in which visible colour change was noted.

Table S2. Calculated limit of detection (LoD) of **L1**@AuNPs

Analyte	**LoD[13]**	**Linear range [μM]**	**Calibration equation [y = $LSPR_{max}$, x = μM]**	**R^2**
Fe^{3+}	11.2	2-7.5	y = 0.708x + 528.59	0.969
Cu^{2+}	9.0	1-7.5	y = 0.88x + 529.12	0.979
Ni^{2+}	-	1-4	y = 1.7x + 528	0.979
	1.4	4-10	y = 5.84x + 511.78	0.989

Real sample analysis

Synthesis of PDE472 intermediate

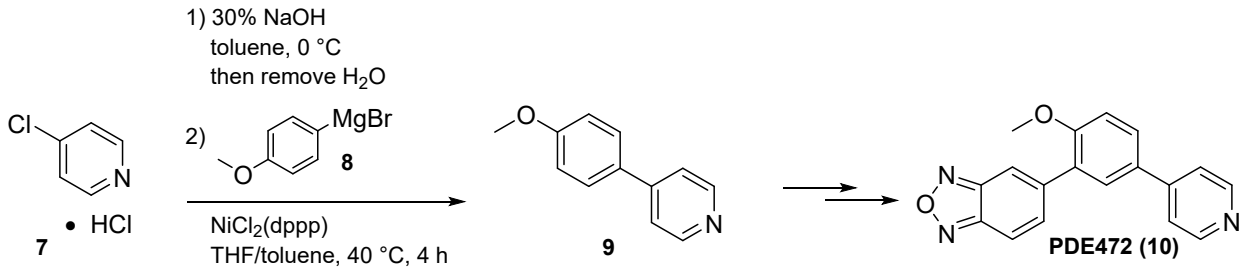

Scheme 4. Synthesis of PDE472 intermediate, via nickel catalysed Kumada coupling[14]

4-(4-Methoxyphenyl)pyridine 9: The intermediate 9 was prepared on a laboratory scale according to the reported procedure.[14]

In detail: 4-bromoanisole (1.5 g, 8.06 mmol) in toluene (1.13 mL) was slowly added in a dropwise manner to Mg turnings (210 mg, 8.62 mmol) and iodine (sublimated, 1.9 mg) activated by heat in THF (3 mL) at 35 °C. After the reaction was initiated, the whole solution was added at such a rate to maintain the temperature of 35 °C. After 3 hours at 45 °C, the mixture was cooled and used for the coupling reaction.

30% NaOH (aqueous solution, 1.05 g, 7.87 mmol) was added to a stirred solution of **7** (1.125 g, 7.5 mmol) in toluene (3.75 mL) and water (4.13 mL) at 0 °C, at such rate that the mixture did not reach more than 5 °C. After another 10 min, the layers were separated and the organic layer was heated under reflux (150 mbar, 50 °C) using a Dean-Stark water trap, for azeotropic water removal. [Safety remark: removal of toluene by distillation can lead to a strongly exothermic autopolymerisation of the free base of **7**]. $NiCl_2$(dppp) (5.6 mg, 0.01 mmol) was then added to the dried base solution of **7** in toluene at ambient temperature. Solution of **8** prepared in the first step

was added dropwise to keep the initial exothermic reaction below 45 °C. After 3 hours at 45 °C reaction was completed, and the mixture was cooled to ambient temperature. Next, a solution of citric acid (1.31 g) in water (2.6 mL) and concentrated HCl (0.38 mL) was prepared, and the reaction mixture was added dropwise over several minutes. The flask was rinsed with toluene (1.13 mL), water (2.63 mL) and concentrated HCl (0.38 mL) and the fractions were added to the reaction mixture. The mixture was then heated to 30 °C and the layers were separated. ***The organic layer, which represents the organic waste from the reaction was put aside for ICP-MS and sensing experiments.*** To the water layer, containing the hydrochloride of **9**, toluene (5.6 mL) and 30 % NaOH (aqueous solution, 3 mL) were added. Layers were separated and the toluene phase was evaporated to dryness, under reduced pressure to yield crude **9**. Spectral data were consistent with the literature.[15] ^{1}H NMR (600 MHz, $CDCl_3$): δ 3.87 (s, 3H), 7.01 (d, 2H, J = 8.7 Hz), 7.47 (d, 2H, J = 6.2 Hz), 7.60 (d, 2H, J = 8.7 Hz), 8.62 (d, 2H, J = 6.2 Hz).

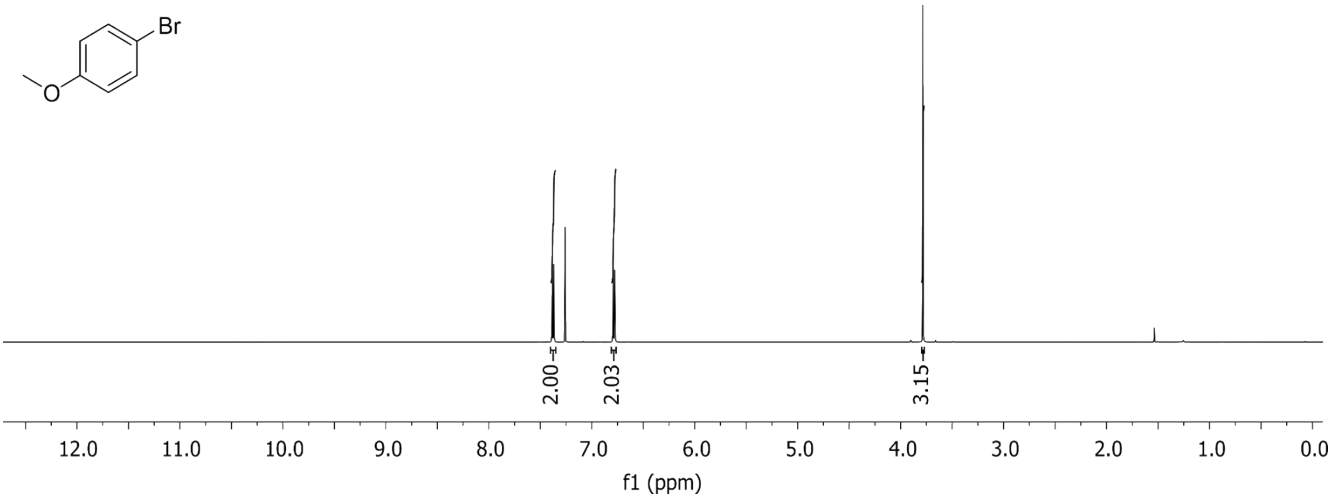

Figure S20. ^{1}H NMR of 4-bromoanisole – substrate to the Kumada coupling leading to **9**, PDE472 intermediate.

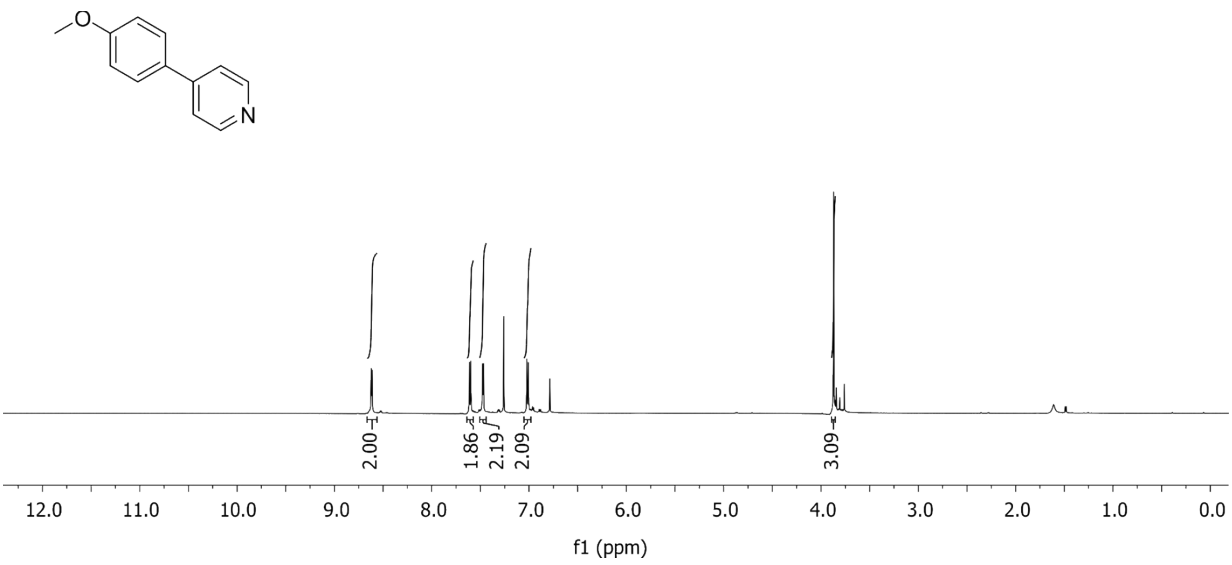

Figure S21. ^{1}H NMR of crude PDE472 intermediate **9**.

Sensing – organic waste sample (Kumada coupling)

Procedure: To 2 mL of gold nanoparticles (in toluene, 0.25 mM in terms of gold metal) different amounts (20-50 µL) of organic waste were added. All spectra were measured at room temperature.

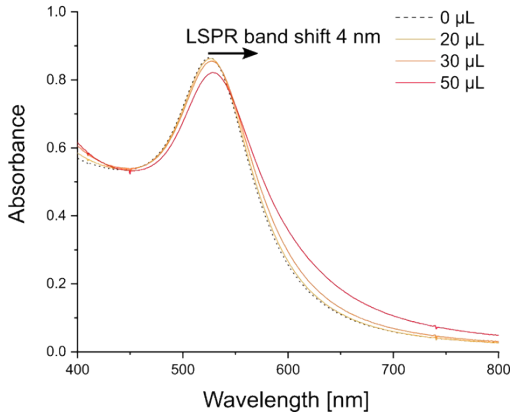

Figure S22. UV-Vis spectra of **L1**@AuNPs upon addition of organic waste.

ICP-MS evaluation of Ni content in organic waste

Sample preparation: 300 µL of organic waste was evaporated under reduced pressure to dryness and was additionally dried under reduced pressure. 50 mg (from resulting 57 mg) of the dried organic waste was mineralized in the following way: The sample digestion was carried out in a microwave-assisted digestion system (Ethos One, Milestone Srl, Italy). About 50 mg of the sample was placed in quartz vessels with 2 mL 65% nitric acid. The digestion program was performed in 3 stages: 20 minutes ramp time to 200 °C, 30 minutes hold time at 200 °C and cooling down for 60 min. The final step in sample preparation was the quantitative transfer of the digested sample to Falcon tubes and 1000-fold dilution with 1% HNO_3.

Evaluation of concentration in organic waste used in sensing experiments: Based on the ICP-MS results (Table S3), Ni^{2+} concentration 44.44 µg/g in 50 mg of solid sample corresponds to 0.143 mM of Ni^{2+} ions in the toluene solution before mineralization. That represents concentration of the solution used for sensing experiments. Adding 50 µL of this stock solution into 2000 µL of **L1**@AuNPs in toluene, result in 3.49 µM Ni^{2+} ion solution.

Table S3. Evaluation of Ni content in organic waste sample determined by ICP-MS (m = weight; c = concentration; SD = standard deviation; CV = coefficient of variation).

m [g]	**c [ug/g]**	**SD [ug/g]**	**CV [%]**
0.050	44.44	0.68	1.5

Time	Sensor	Analyte	Reference
10 min	Phyto extract GNP	Cd(II)	[16]
NR (rapid)	Schiff base GNP	Hg(II)	[17]
10 sec	Schiff base GNP	Al(III)	[18]
20 sec	Nitriloacetic acid and His GNP	Ni(II)	[19]
1 min	Cys GNP	Sc(III)	[20]
NR	Schiff base GNP	Fe(III)	[21]
NR (rapid)	Vitamin B6 GNP	Cr(III)	[22]
20 min	Mo hydrogel	As(III)	[23]
6 min	GSH and Cys Silver nanoplates	Ni(II)	[24]
95 min	Schiff base	Fe(III)	[25]
10 min	PAM AgBr NCs	Pb(II), Cu(II)	[26]
1 min	Peptide GNP	Co(II), Hg(II), Pb(II), Pd(II), Pt(II)	[27]

Table S4. Response time for colorimetric sensors.

NR = not reported

References:

1. R. J. Stokes, A. Macaskill, J. A. Dougan, P. G. Hargreaves, H. M. Stanford, W. E. Smith, K. Faulds and D. Graham, *Chem Commun,* 2007, DOI: 10.1039/b705873j, 2811-2813.
2. N. E. Pollok, C. Rabin, L. Smith and R. M. Crooks, *Bioconjug Chem*, 2019, **30**, 3078-3086.
3. *USA Pat.,* US2008/286607, 2008.
4. A. J. Fugard, B. K. Thompson, A. M. Slawin, J. E. Taylor and A. D. Smith, *Org Lett*, 2015, **17**, 5824-5827.
5. A. M. Johnson, M. C. Young, X. Zhang, R. R. Julian and R. J. Hooley, *J Am Chem Soc*, 2013, **135**, 17723-17726.
6. M. R. Baumgartner, H. Schmalle and E. Dubler, *Inorganica Chim Acta*, 1996, **252**, 319-331.
7. H. Sigel, B. Prijs and D. B. McCormick, *J Inorg Nucl Chem*, 1978, **40**, 1678-1680.
8. X. Huang, A. J. Shumski, X. Zhang and C. W. Li, *J Am Chem Soc*, 2018, **140**, 8918-8923.
9. V. Montes-García, S. Rodal-Cedeira, M. J. Cordero-Ferradás, B. Gómez, L. García-Río, I. Pastoriza-Santos and J. Pérez-Juste, *Isr J Chem*, 2018, **58**, 1251-1260.
10. M. J. Hostetler, J. E. Wingate, C.-J. Zhong, J. E. Harris, R. W. Vachet, M. R. Clark, J. D. Londono, S. J. Green, J. J. Stokes, G. D. Wignall, G. L. Glish, M. D. Porter, N. D. Evans and R. W. Murray, *Langmuir*, 1998, **14**, 17-30.
11. X. Liu, M. Atwater, J. Wang and Q. Huo, *Colloids Surf B Biointerfaces*, 2007, **58**, 3-7.

12. J. C. Love, L. A. Estroff, J. K. Kriebel, R. G. Nuzzo and G. M. Whitesides, *Chem Rev*, 2005, **105**, 1103-1169.
13. X. Jia, D. Chao, L. He, H. Liu, T. Zheng, C. Zhang and C. Wang, *Macromol Res*, 2011, **19**, 1127-1133.
14. P. W. Manley, M. Acemoglu, W. Marterer and W. Pachinger, *Org Process Res Dev*, 2003, **7**, 436-445.
15. S. Panda, A. Coffin, Q. N. Nguyen, D. J. Tantillo and J. M. Ready, *Angew Chem Int Ed Engl*, 2016, **55**, 2205-2209.
16. K. Singh, V. Kumar, B. Kukkar, K. H. Kim and T. R. Sharma, *Int J Environ Sci Technol*, 2021, DOI: 10.1007/s13762-021-03331-0.
17. F. Amourizi, K. Dashtian, M. Ghaedi and B. Hosseinzadeh, *Anal Methods*, 2021, **13**, 2603-2611.
18. P. Huang, J. Li, X. Liu and F. Wu, *Microchim Acta*, 2015, **183**, 863-869.
19. Z. Krpetic, L. Guerrini, I. A. Larmour, J. Reglinski, K. Faulds and D. Graham, *Small*, 2012, **8**, 707-714.
20. H.-H. Deng, K.-Y. Huang, Q.-H. Fang, Y.-P. Lv, S.-B. He, H.-P. Peng, X.-H. Xia and W. Chen, *Sens Actuators B Chem*, 2020, **311**, 127925.
21. A. A. Jimoh, A. Helal, M. N. Shaikh, M. Abdul Aziz, Z. H. Yamani, A. Al-Ahmed and J.-P. Kim, *J Nanomater*, 2015, **2015**, 1-7.
22. Y. Upadhyay, S. Bothra, R. Kumar and S. K. Sahoo, *ChemistrySelect*, 2018, **3**, 6892-6896.
23. J. Das and P. Sarkar, *Environ Sci Water Res Technol*, 2016, **2**, 693-704.
24. T. Kiatkumjorn, P. Rattanarat, W. Siangproh, O. Chailapakul and N. Praphairaksit, *Talanta*, 2014, **128**, 215-220.
25. T.-B. Wei, P. Zhang, B.-B. Shi, P. Chen, Q. Lin, J. Liu and Y.-M. Zhang, *Dyes Pigm*, 2013, **97**, 297-302.
26. A. K. Yetisen, Y. Montelongo, M. M. Qasim, H. Butt, T. D. Wilkinson, M. J. Monteiro and S. H. Yun, *Anal Chem*, 2015, **87**, 5101-5108.
27. J. M. Slocik, J. S. Zabinski, Jr., D. M. Phillips and R. R. Naik, *Small*, 2008, **4**, 548-551.